machines

MDPI

Article

Simulation of Load–Sinkage Relationship and Parameter Inversion of Snow Based on Coupled Eulerian–Lagrangian Method

Ming Zhu [1], Pengyu Li [2,3], Dongqing Li [2], Wei Wei [1,3,*], Jianfeng Liu [3], Xixing Long [1,3], Qingkai Meng [1], Yongjie Shu [1] and Qingdong Yan [1,3]

[1] School of Mechanical Engineering, Beijing Institute of Technology, Beijing 100081, China; 3220205057@bit.edu.cn (M.Z.); 3120205193@bit.edu.cn (Q.Y.)
[2] Harbin First Machinery Group Co., Ltd., Harbin 150001, China
[3] Chongqing Innovation Center, Beijing Institute of Technology, Chongqing 401120, China; 3220220426@bit.edu.cn
* Correspondence: weiweibit@bit.edu.cn

Abstract: The accurate calibration of snow parameters is necessary to establish an accurate simulation model of snow, which is generally used to study tire–snow interaction. In this paper, an innovative parameter inversion method based on in situ test results is proposed to calibrate the snow parameters, which avoids the damage to the mechanical properties of snow when making test samples using traditional test methods. A coupled Eulerian–Lagrangian (CEL) model of plate loading in snow was established; the sensitivity of snow parameters to the macroscopic load–sinkage relationship was studied; a plate-loading experiment was carried out; and the parameters of snow at the experimental site were inverted. The parameter inversion results from the snow model were verified by the experimental test results of different snow depths and different plate sizes. The results show the following: (1) The material cohesive, angle of friction, and hardening law of snow have great influence on the load–sinkage relationship of snow, the elastic modulus has a great influence on the unloading/reloading stiffness of snow, and the influence of density and Poisson's ratio on the load–sinkage relationship can be ignored. (2) The correlation coefficient between the inversion result and the matching test data is 0.979, which is 0.304 higher than that of the initial inversion curve. (3) The load–sinkage relationship of snow with different snow depths and plate diameters was simulated by using the model parameter of inversion, and the results were compared with the experimental results. The minimum correlation coefficient was 0.87, indicating that the snow parameter inversion method in this paper can calibrate the snow parameters of the test site accurately.

Keywords: load–sinkage relationship; parameter inversion; MDPC; coupled Eulerian–Lagrangian method

check for updates

Academic Editor: Khalil Khanafer

Received: 24 September 2024
Revised: 24 November 2024
Accepted: 26 November 2024
Published: 25 December 2024

Citation: Zhu, M.; Li, P.; Li, D.; Wei, W.; Liu, J.; Long, X.; Meng, Q.; Shu, Y.; Yan, Q. Simulation of Load–Sinkage Relationship and Parameter Inversion of Snow Based on Coupled Eulerian–Lagrangian Method. *Machines* **2025**, *13*, 8. https://doi.org/10.3390/machines13010008

Copyright: © 2024 by the authors. Licensee MDPI, Basel, Switzerland. This article is an open access article distributed under the terms and conditions of the Creative Commons Attribution (CC BY) license (https://creativecommons.org/licenses/by/4.0/).

1. Introduction

The interaction between the wheel/track and soft ground directly affects the driving performance of wheeled/tracked vehicles running on soft terrain. In order to obtain a deep understanding of the interfacial characteristics between the wheel/track and soil, scholars have conducted experimental and simulation research [1–6] using soil bin test systems. However, the mechanical properties of snow are more complex than those of soil. Experimental studies on the interfacial performance between wheels/tracks and snow based on the soil bin system are limited because it is difficult to guarantee the

snow environment, and the simulation research is limited because of the lack of a feasible snow model.

Snow is a kind of porous/multiphase material whose mechanical properties are affected by light and the water content, temperature, and crystal structure of snow. A series of mechanical tests conducted by the Cold Region Research and Engineering Laboratory [7–11] (CRREL) on snow showed that the strength of the snow increased 10-fold after 6 days of sintering, and the shear index was irregularly related to the temperature and crystal size of the snow. In the density range of 900 kg/m^3, the elastic modulus of snow changes by four orders of magnitude, and the bearing capacity of the elastic part of snow on a vehicle can be ignored when the density of the snow is below 300 kg/m^3. Based on the experimental data of snow mechanical properties conducted by CREEL, Sally Shoop [11,12] analyzed a plastic model of snow in detail and calibrated the parameters of the snow with a density of 200 kg/m^3. Jonah H analyzed the stress distribution of snow under the interaction between wheel and snow based on the Modified Drucker–Prager Cap model [13], and verified the theoretical model using simulation results of the interaction between wheel and snow in the absence of relevant experimental data [14,15]. The traction force and motion resistance of patterned tires running in snow were simulated, and the interfacial characteristics between the patterned tires and snow with different model parameters was compared by Choi, J. H [16] using the FEM-FVM coupling simulation method.

However, the mechanical properties of snow used in the above numerical simulation are not consistent with those of actual snow. In order to reflect the mechanical properties of snow in different regions, temperatures, and sintering times, the model parameters need to be further studied and redefined. Some methods for calibrating soil parameters can be used for reference. Soil model parameters including cohesion, internal friction angle, saturation, and density need to be obtained using appropriate testing methods, such as laboratory experiments, triaxial experiments, direct shear experiments, in situ tests, and cone penetration tests. These selected methods should produce results as close as possible to the field values and provide all of the data necessary for the numerical simulation, such as continuum-based numerical techniques and discrete-based numerical techniques [17,18]. In order to solve the problem of slope failure, Huang and Fei made a soil cylinder sample in the laboratory and tested the shear strength of unsaturated soil through triaxial experiments [19]. In order to calibrate the parameters of the DEM of simulated lunar soil, Jianzhong Zhu conducted conical pile experiment tests and calibrated the angle of repose. Penetration tests were conducted to verify the accuracy and validity of the DEM parameters [20]. In order to test the interaction behavior between a small-wheeled mobile platform tire and forest soil, Liyang Yao established the FEM-DEM simulation model, in which soil parameters were obtained through standard geotechnical tests and uniaxial experiments [21]. However, whether these methods suitable for testing soil parameters are suitable for testing snow parameters remains to be studied because of the limited bearing capacity of snow and the difficulty of obtaining snow experiment samples.

The in situ test of soft ground can maintain the mechanical properties of undisturbed soft ground as much as possible and can provide more accurate results than laboratory test results. Parameter inversion is a common method used to calibrate soft ground parameters by using in situ test results. Zhu Min conducted a parameter inversion of the relevant parameters of the hardened soil model based on a self-drilling side-pressure experiment curve, and obtained the value range of the parameters of the hardened soil model for finite element simulation analysis [22]. The Duncan–Chang model is used to establish the finite element model of soil in the foundation cover layer. Based on the sensitivity analysis of each parameter of the model, Liu Xiaosheng took the laboratory test results as the initial values to invert the soil parameters in the foundation cover layer. Compared with the

traditional laboratory soil sample test results, the parameter inversion results are closer to the in situ test results [23]. Rangeard D. calibrated the parameters of the Cam–Clay model using the parameter inversion method [24]. However, no investigation has been conducted into the back-analysis of snow parameters based on the in situ test results.

In addition, machine learning may also be an effective method to calibrate the parameters of soft terrain models, but the application of machine learning-based methods in the calibration of snow parameters in the area of snow thickness and temperature calibration has not been reported in the literature. For example, Yao Heming proposes a novel inverse method based on the deep convolutional neural network to extract data on the layer thickness and temperature of snow via passive microwave remote sensing [25], and Junyu Zhan proposed a novel global navigation satellite system–interferometric reflectometry signal-to-noise ratio-retrieving snow depth method to monitor the depth of snow [26]. Deep learning technology in the field of soil is mainly applied in soil classification, soil image processing, soil terrain recognition, etc., and is less applied in soil mechanic parameter calibration.

The accuracy of a snow model directly affects the simulation results of wheeled/tracked vehicle driving performance in snow. In this paper, an innovative method of parameter inversion based on in situ test results of the load–sinkage relationship of snow is proposed to calibrate snow parameters: A finite element model of plate loading was established to analyze the sensitivity of snow parameters to the load–sinkage relationship, the snow parameters with greater sensitivity were selected and calibrated based on the in-situ test results of load–sinkage relationship. Compared with the traditional experimental method for measuring the mechanical properties of soft terrain, as shown in Table 1, the parameter inversion method proposed in this paper, which avoids the destruction of undisturbed snow when obtaining experimental samples, is more suitable for the measurement of snow parameters.

Table 1. Comparison of calibration methods for mechanical parameters of soft ground.

Calibration Method	Experimental Object	Calibration Item	Experimental Sample
triaxial testing	red clay [19], forest soil [21], dam base gravel [23], soil [27,28]	shear strength [6,19], contact model parameters in DEM [21,28], parameters for Duncan–Chang model in FEM [23], shear failure and cap yield surface in MDPC model [27,29]	• cylindrical sample [6,19,21,23,27–30], • conical pile of soil rather than experimental samples [20,31], • soil bin test sample [6], • in situ test (no experimental samples) [32]
uniaxial loading	soil [27,30]	Young's modulus and Poisson's ratio [27]	
direct shear	paddy soil [6]	failure surface parameters of MC model [30]	
penetration test	paddy soil [6]	parameters of Bekker model [6]	
compaction test	paddy soil [6]	bearing capacity of the soil [6]	
repose angel test	sandy soil [31]	interaction coefficients of Hertz–Mindlin model [31]	
Box–Behnken experiment	lunar soil simulant [20]	Hertz–Mindlin contact model parameters in DEM [20]	
self-boring test and back-analysis	granite residual soil [32]	parameters of hardening soil model in FEM [32]	
bearing capacity in situ test and parameter inversion (proposed in this paper)	snow	load–sinkage relationship	in situ test (no experimental samples)

2. Plate-Loading Experiment

2.1. Bearing Model of Snow

The load–sinkage relationship of soft terrain is generally determined by the circular plate-loading experiment. In the semi-finite snow environment, the stress distribution of snow under circular plate loading cannot be affected by the hard terrain underneath the snow, and the load–sinkage relationship can be expressed as Equation (1) [33]:

$$F = A\left(\frac{k_c}{b} + k_\varphi\right) z^n \quad (1)$$

where A is the area of the circular plate (m^2); k_c is the cohesive deformation modulus of snow (kPa/m^{n+1}); b is the radius of plate (m); k_φ is the friction deformation modulus of snow (kPa/m^n); z is the snow sinkage (m); and n is the deformation index of snow.

However, the bearing capacity of the snow is limited, and snow deformation is large under the vertical load of the vehicle. The stress distribution of snow can be affected considerably by the hard terrain beneath the snow. Therefore, the load–sinkage relationship considering the snow depth can be expressed by Equation (2) [34]:

$$F = Ap_w\left[-\ln\left(1-\frac{z}{z_w}\right)\right] \tag{2}$$

where z_w is the height parameter of the soft terrain, which is generally its depth; and p_w is the pressure parameter, which is generally selected when the sinkage is 93% of the depth of the soft terrain.

In the process of vehicle running, the largest proportion of snow deformation is plastic deformation, and only a small part is elastic deformation. Snow undergoes the cyclic stress state of loading, unloading, and reloading when the front and rear wheels of a wheeled vehicle or the roadwheels of a tracked vehicle pass in sequence. If unloading occurs when the sinkage is z_u, and the sinkage in the reloading stage is less than z_u, the load–sinkage relationship in the unloading/reloading stage can be expressed by Equation (3) [34]:

$$F = \mathrm{A}\left\{p_w\left[-\ln\left(1-\frac{z_u}{z_w}\right)\right]+k_u(z-z_u)\right\} \tag{3}$$

where z_u is the sinkage at the beginning of unloading, and k_u is the unloading stiffness.

2.2. Experimental Process

A snow test system was designed to measure the load–sinkage relationship of snow during loading, unloading, and reloading, as shown in Figure 1. The test system includes a support frame, force sensor, displacement sensor, counterweight, circular plate, and upper computer. The data acquisition frequency is 10 Hz. The counterweights are hung by hooks on the support frame. With eight counterweights (each of which is about 18.5 kg) suspended on the support frame, together with the mass of the support frame, the test range of the test system is up to approximately 1600 N.

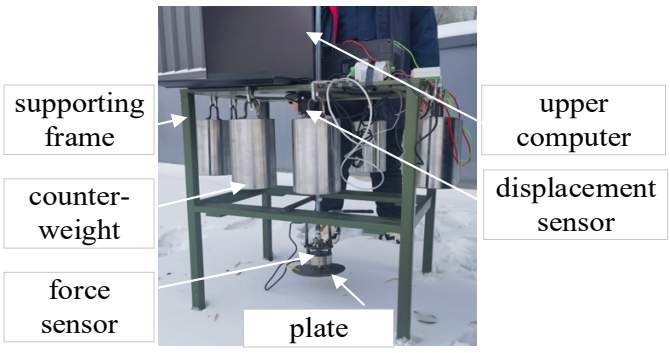


Figure 1. Test system of load–sinkage relationship of snow.

The test system is loaded through the screw, and the vertical velocity of the circular plate is about 2 mm/s. When the vertical displacement of the circular plate is large enough and the vertical force of the terrain acting on the circular plate is greater than the maximum load of the test system, the supporting frame will shake and the loading process is completed.

Three circular plates of different sizes, with diameters of 0.10 m, 0.14 m, and 0.18 m, were used during test process in snow with depths of 0.14 m, 0.18 m, and 0.20 m, respectively, in Harbin. The snow was natural snowfall, the natural static sintering time was about 7 days, and the temperature during the test was about −4 °C.

3. MDPC Snow Model

Snow is a porous polyphase material, whose plastic deformation can be simulated using the Mohr–Coulomb model, Drucker–Prager model, Modified Drucker–Prager Cap model, etc. Compared with the Mohr–Coulomb model and the Drucker–Prager model, the Modified Drucker–Prager Cap (MDPC) plastic model can more realistically simulate the plastic deformation of snow by adding a material yield criterion caused by isotropic compression. According to Ref. [11], the yield surface of the MDPC plastic model is described by the stress invariant in the stress tensor, which can be expressed as Equations (4)–(6):

$$p = -\sigma_{oct} = -\frac{1}{3}\boldsymbol{\sigma} : \mathbf{I} \tag{4}$$

$$q = \sqrt{\frac{3}{2}(\mathbf{S} : \mathbf{S})} \tag{5}$$

$$r = \left(\frac{9}{2}\mathbf{S}\cdot\mathbf{S} : \mathbf{S}\right)^{\frac{1}{3}} \tag{6}$$

where p is the equivalent stress, q is the deviator stress, r is the third stress invariant, and **S** is the stress deviator tensor, where **S** = **σ** + p**I**. The combination of the second and third stress invariants forms a new invariant expression, as in Equation (7):

$$t = \frac{q}{2}\left[1 + \frac{1}{K} - \left(1 - \frac{1}{K}\right)\left(\frac{r}{q}\right)^{3}\right] \tag{7}$$

where K is the stress flow potential (the ratio between the tensile stress and the compressive stress) and describes the yield surface in the deviator stress plane. When K = 1, the yield surface is circular, and the tensile yield stress and compressive yield stress are equal. When K = 0.778, the model can approximately describe the Mohr–Coulomb yield surface, as shown in Figure 2.

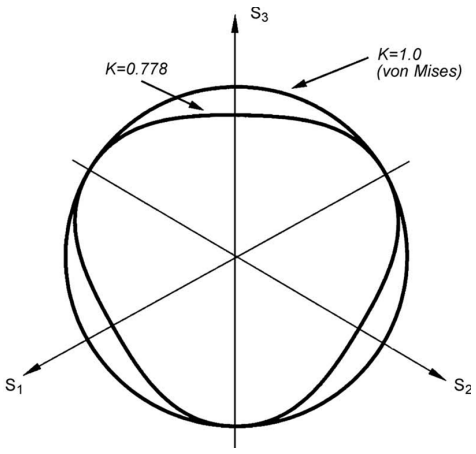


Figure 2. Modified Drucker–Prager yield surface in deviatoric space [35].

The yield surface of the MDPC plastic model can be expressed in the p-t plane, as shown in Figure 3, which includes shear yield surface, Cap yield surface, and transition surface, which can be expressed by Equations (8)–(10), respectively.

$$F_s = t - ptan\beta - d = 0 \tag{8}$$

$$F_c = \sqrt{(p - p_a)^2 + \left[\frac{Rt}{\left(1 + \alpha - \frac{\alpha}{cos\beta}\right)}\right]^2} - R(d + p_a tan\beta) = 0 \tag{9}$$

$$F_t = \sqrt{(p - p_a)^2 + \left[t - \left(1 - \frac{\alpha}{cos\beta}\right)(d + p_a tan\beta)\right]^2} - \alpha(d + p_a tan\beta) = 0 \tag{10}$$

where d is the material cohesion, β is the angle of friction, α is the transition surface coefficient, R is the Cap eccentricity, p_a is the intersection point of shear yield surface and Cap yield surface, and p_b is the hydrostatic pressure (p_b is a function of the volumetric plastic strain ε_{vol}^{pl}, $p_b = f\left(\varepsilon_{vol}^{pl}\right)$), which defines the hardening law during compression.

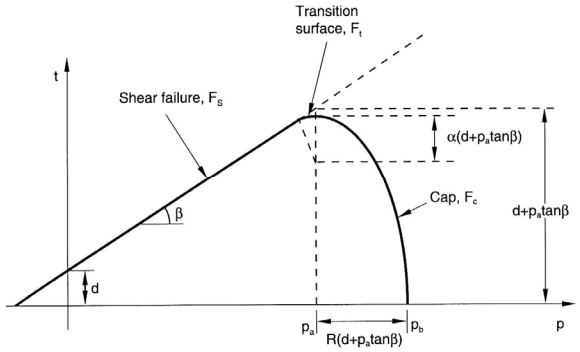


Figure 3. Modified Drucker–Prager Cap yield surface in the p-t plane [35].

When the stress state of snow reaches the initial yield surface, it is necessary to use the stress flow potential to describe the relationship between the plastic strain increment tensor and the plastic stress increment tensor. As shown in Figure 4, when the non-correlated plastic flow potential is applied to the shear yield surface and the correlated plastic flow potential is applied to the Cap yield surface, the stress flow potential surface can be expressed as Equation (11) and Equation (12), respectively.

$$G_s = \sqrt{[(p - p_a)\ tan\beta]^2 + \left[\frac{t}{\left(1 + \alpha - \frac{\alpha}{cos\beta}\right)}\right]^2} \tag{11}$$

$$G_c = \sqrt{(p - p_a)^2 + \left[\frac{Rt}{\left(1 + \alpha - \frac{\alpha}{cos\beta}\right)}\right]^2} \tag{12}$$

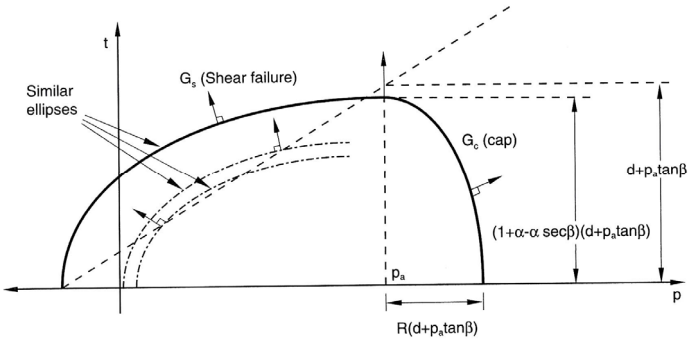


Figure 4. The plastic flow potential [35].

4. Snow Parameter Inversion

The cohesive force, angle of friction, elastic modulus, and hardening law of the model should be calibrated based on triaxial experiments and direct shear experiments, which have been widely used in soil mechanics [28,31]. As for snow, its bearing capacity is limited, and its mechanical properties are greatly affected in the process of obtaining experimental samples, which leads to experimental test results that are far from the original values. Therefore, an innovative method for the parameter inversion of snow model parameters based on the in situ test results of the load–sinkage relationship of snow is proposed in this paper, as shown in Figure 5. This method avoids the disturbance of snow during the preparation of the experimental samples, which leads to inaccurate parameter calibration results.

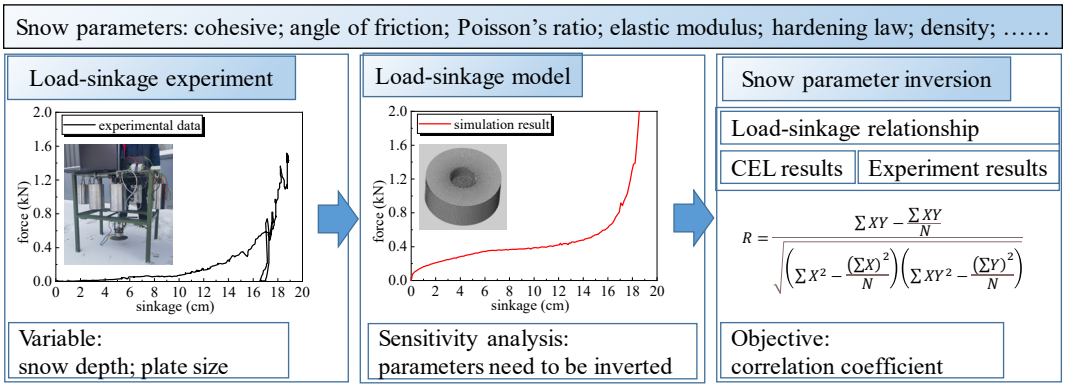


Figure 5. The parameter inversion method proposed in this paper.

4.1. Simulation Model

The simulation model of circular plate loading in snow was established, and the MDPC model was used to describe the plastic deformation of snow. The plate diameter was 0.1 m and the snow depth was 0.2 m (the same as the experimental condition above). According to the relevant literature and simulation results, when the snow radius is greater than two times the circular plate radius, the snow boundary will not be deformed. Thus, the snow radius was 0.125 m.

The snow under circular plate loading will have large plastic deformation, which will cause great difficulty in the convergence of the simulation [36]. In the simulation of the interaction between wheel and snow, Jonah H. Lee improved the mesh quality in the simulation process using the Arbitrary Lagrange–Eulerian (ALE) method [14]. The ALE method can re-mesh the geometry when the mesh is distorted. However, the situation still exists in which the simulation process is aborted due to poor mesh quality. The wide applicability of the ALE method is limited, especially in the simulation of tracked vehicles running on snow.

The coupled Eulerian–Lagrangian (CEL) method is an effective method to solve the large deformation problem [37,38]. The snow material flows freely in the Euler region, and the mesh does not deform. Therefore, the Euler region of the snow was established, and the snow depth was 0.2 m, as shown in Figure 6. The model parameters of the snow are shown in Table 2.

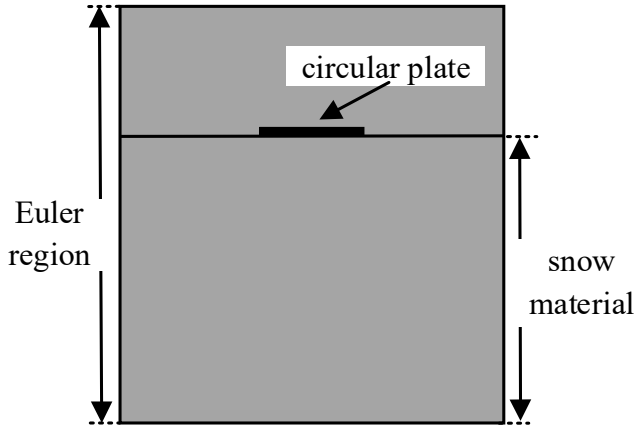


Figure 6. Simulation model of circular plate loading in snow.

Table 2. Material parameters of snow MDPC.

Elastic	*** Young's modulus** E/(Pa)		*** Poisson's ratio** ν	*** Density** ρ/(kg·m^{-3})		
	1.379×10^6		0.3	200		
Plastic	*** Cohesion** c/(Pa)	*** Angle of friction** β/deg	**Cap eccentricity**	**Initial yield surface position** $\varepsilon_{vol}^{pl}\|_{initial}$	**Transition surface radius**	**Flow stress ratio**
	5000	22.53	0.00011	0.001	0	1
*** Cap hardening**				ε_{vol}^{pl}	Mean hydrostatic pressure/Pa	
				0	113.76	
				0.593	17,000	
				0.669	33,000	
				0.806	67,000	
				0.944	167,000	
				1.083	333,000	
				1.299	667,000	
				1.455	933,000	
				1.475	1,083,000	
				1.5	2,000,000	
				1.514	20,000,000	

The simulation process lasts for 96 s and the sinkage of the circular plate is 0.185 m (the same as in the experiment). When the circular plate moves down a certain distance, the circular plate is unloaded, and the unloading displacement is 10 mm (at this distance, the elastic deformation of the snow is completely restored, and the unloading/reloading stiffness of the snow can be calculated).

4.2. Sensitivity Analysis of Snow Parameters

The sensitivity of the snow model parameters to the load–sinkage relationship of snow was analyzed by means of a single-factor sensitivity analysis method in this paper. Taking the snow parameters in Table 1 as the comparison group, the parameters marked with * were changed separately, with the other parameters unchanged (30%, 60%, 130%, and 160% of each variable to be changed were taken as the experimental group, with a total of 24 experimental groups). Circular plate-loading simulations were carried out on each sample to analyze the sensitivity of each variable to the load–sinkage relationship and unloading stiffness.

4.3. Parameter Inversion of Snow Model Parameters

In the process of inverting the snow parameters, the load–sinkage relationship of snow obtained from the in situ test in Section 2.2 was used as the matching data. The model parameter closest to the experimental test result in the sensitivity analysis was taken as the initial value of the parameter inversion, the maximum correlation coefficient between the test result and the simulation result of the load–sinkage relationship was taken as the objective function, and the model parameters were searched by the NSGA-II optimization algorithm. The correlation coefficient can be expressed as Equation (13):

$$R = \frac{\sum XY - \frac{\sum X \sum Y}{N}}{\sqrt{\left(\sum X^2 - \frac{(\sum X)^2}{N}\right)\left(\sum XY^2 - \frac{(\sum Y)^2}{N}\right)}} \tag{13}$$

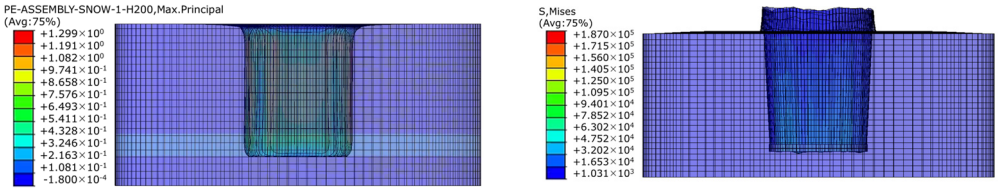
where X is the experimental result and Y is the simulation result. The range of the correlation coefficient R is $[-1\ 1]$. When $R = 0$, X and Y have no correlation; when $|R| = 1$, there is a linear function relationship between X and Y. When $|R| < 1$, the change in X will cause the change in Y. The greater the absolute value of R, the greater the change in Y caused by the change in X. When $|R| > 0.8$, the correlation between the two is strong.

The NSGA-II algorithm is a genetic algorithm based on the Pareto optimization concept, which includes fast non-dominated sorting, an individual crowding distance operator design, and an elite retention strategy. The NSGA-II used was set as follows: crossover probability 0.91, genetic algebra 63, initial population size 27, crossover index 10, variation distribution index 20, and a total of 1200 iterations. In the process of parameter inversion, the initial value of the model parameters is used to simulate the load–sinkage relationship, and then the objective function under the model parameters is calculated. When the objective function under the parameter is less than the given optimization termination condition, the model parameters are adjusted according to the NSGA-II optimization method, and the load–sinkage relationship under the new model parameters are re-simulated. When the objective function under this parameter is greater than the given optimization termination condition or reaches the given number of iterations, the simulation ends.

5. Results

5.1. Advantages of CEL

The snow deformation under circular plate loading is shown in Figures 7 and 8. The simulation method based on Lagrange results in serious mesh distortion and the interruption of the simulation with large snow deformation. The simulation method based on CEL can effectively simulate large snow deformation. From the snow deformation experimental and simulation results, the CEL-based snow deformation results are more consistent with the actual situation.



(**a**) (**b**)

Figure 7. Snow deformation results under different simulation methods ((**a**): CEL; (**b**): Lagrange).

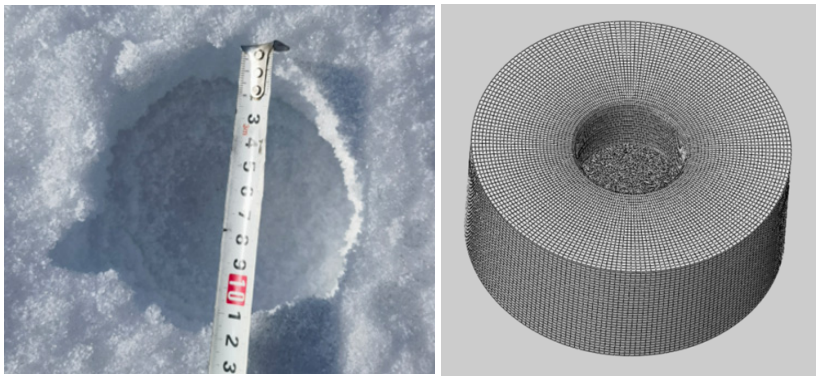


Figure 8. Experimental and simulation results of snow deformation.

5.2. Sensitivity Analysis Result

It can be seen from the sensitivity results of the model parameters to the load–sinkage relationship of snow (as shown in Figure 9) that the material cohesion, angle of friction, and the hardening law of snow have great influence on its load–sinkage relationship, while the density, Poisson's ratio, and elastic modulus have little influence. The elastic modulus of snow has a great influence on the unloading stiffness, while the other parameters have little impact.

In contrast to the load–sinkage results of the comparison group, the force change rate caused by the experimental group is shown in Figure 10. The increase in material cohesion, angle of friction, and hardening law results in the increase in the snow load with the same sinkage. With the increasing angle of friction, the force change rate increases with the increasing plate sinkage. When the angle of friction increases by 60%, the snow load increases the most when the circular plate is close to the snow bottom, which is 168.9%. When the circular plate is close to the snow bottom, the influence of the hardening law on the snow load decreases. The influence of elastic modulus, Poisson's ratio, and density on the load–sinkage relationship of snow is relatively limited.

As for the unloading stiffness of the snow, the unloading stiffness of the comparison group is 534.025 kN/m, and the unloading stiffness of the snow with various parameter changes is shown in Figure 11. Among them, the elastic modulus of snow has the greatest influence on the unloading stiffness. When the elastic modulus is changed to 30% and 130% of the comparison group, the unloading stiffness changes by 60.7% and 69.45%, respectively, while the largest change rate of unloading stiffness caused by the other parameters is 9.6%. Therefore, it can be considered that the unloading stiffness of snow is only affected by the elastic modulus, and the change in the elastic modulus only affects the unloading stiffness of snow. When the plate diameter is 0.1 m and the snow depth is 0.2 m in the experimental condition, the unloading stiffness of the snow is about 689.537 kN/m. According to the relationship between elastic modulus and unloading stiffness in Figure 9, the elastic modulus of the test snow was 121% of that of comparison group, which was 1.669 Mpa.

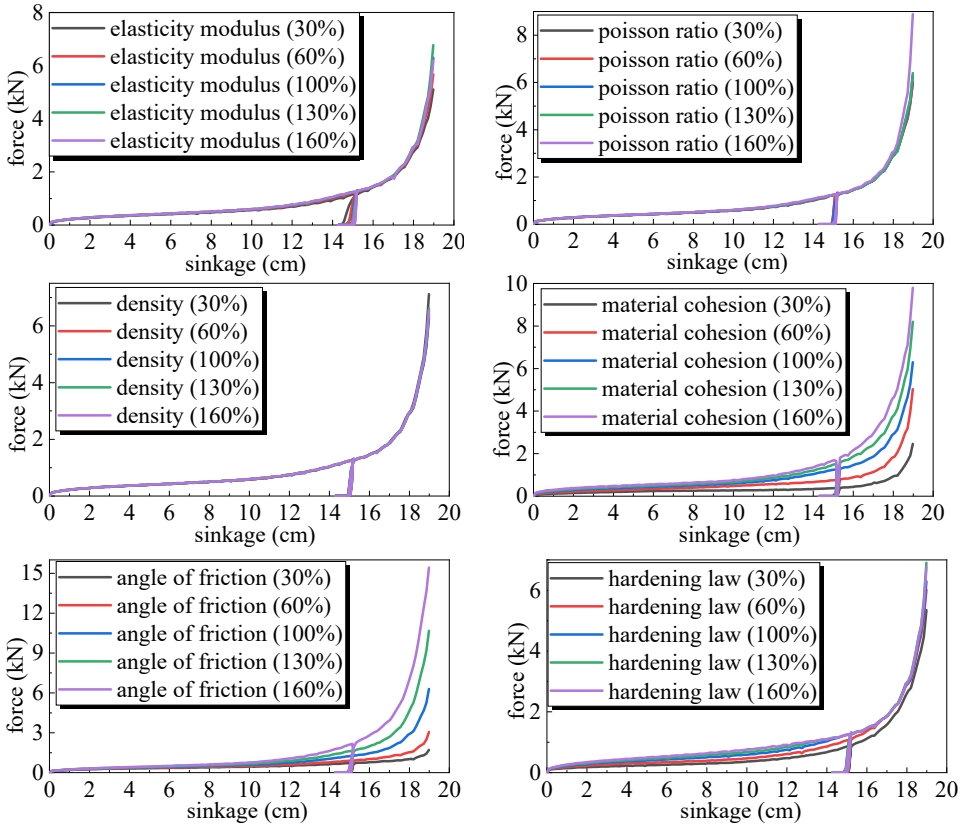


Figure 9. Influence of snow parameters on load–sinkage relationship.

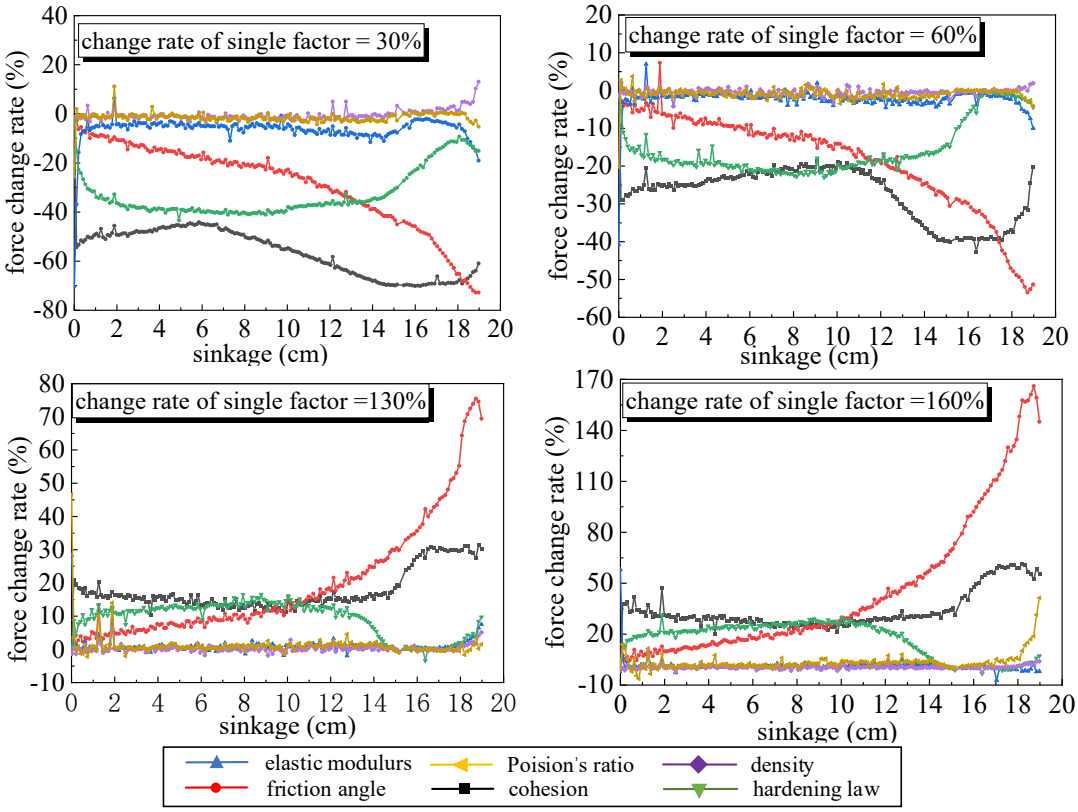


Figure 10. Force change rate during continuous loading with single-factor change.

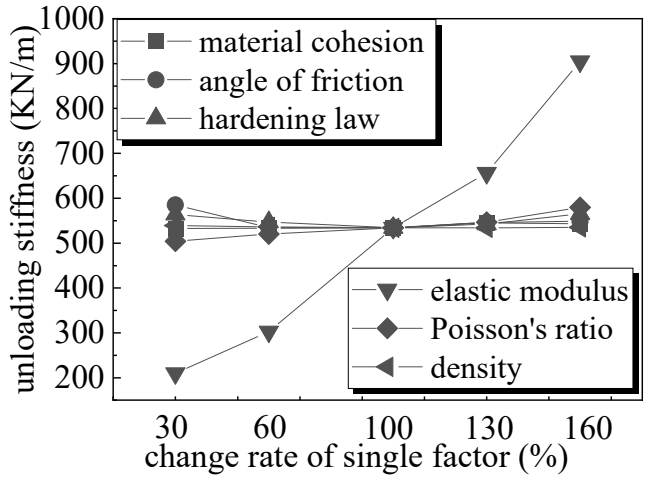


Figure 11. Influence of snow parameters on unloading stiffness.

5.3. Parameter Inversion Results

It can be seen from the snow parameter sensitivity analysis that the elastic modulus of snow corresponds to the unloading stiffness one-by-one. In order to simplify the process of parameter inversion, only the load–sinkage relationship under continuous loading is used for parameter inversion, with the unloading process being ignored. In the case that the elastic modulus of snow has been calibrated, only the material cohesion, angle of friction, and hardening law of snow need to be inverted.

When the plate diameter is 0.1 m and the snow depth is 0.2 m, the experimental result, the matching data, the inversion initial curve, and the inversion result curve are as shown in Figure 12. The experimental data for the load–sinkage in the continuous loading stage are selected as the matching curve of parameter inversion, and the curve closest to the experimental data is selected from the sensitivity analysis results as the initial curve of parameter inversion. The correlation coefficient between the initial inversion curve and the experimental data is 0.675. The inversion result curve has a high fit with the experimental data, and the correlation coefficient is 0.979, which is increased by 0.304.

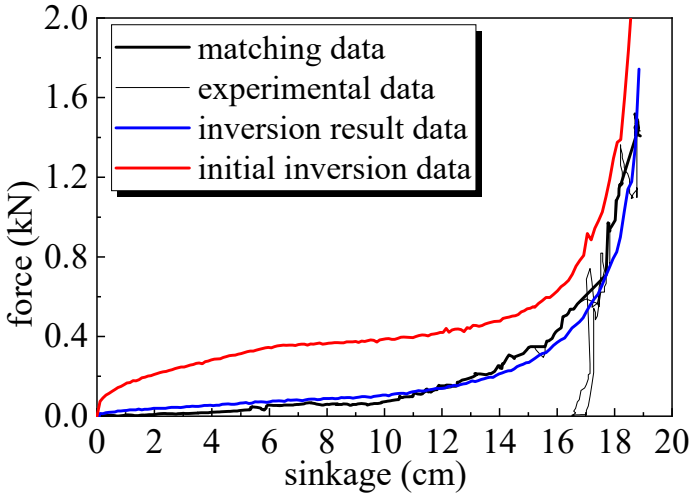
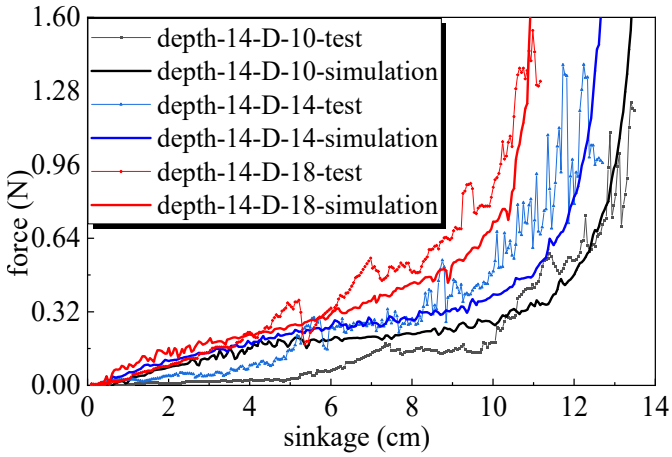
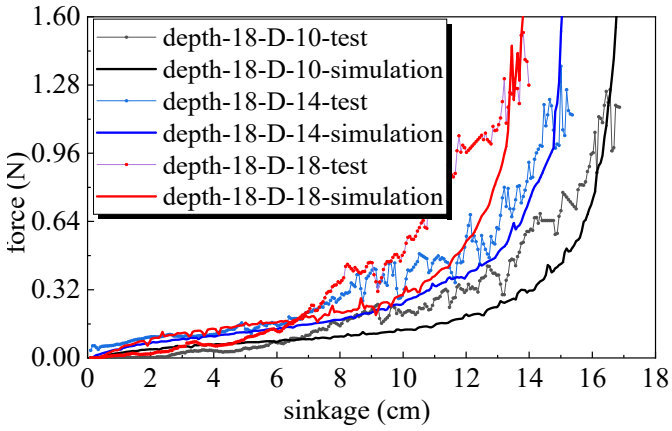


Figure 12. Comparison of load–sinkage results of snow (load–sinkage relationship before and after parameter inversion and test data).

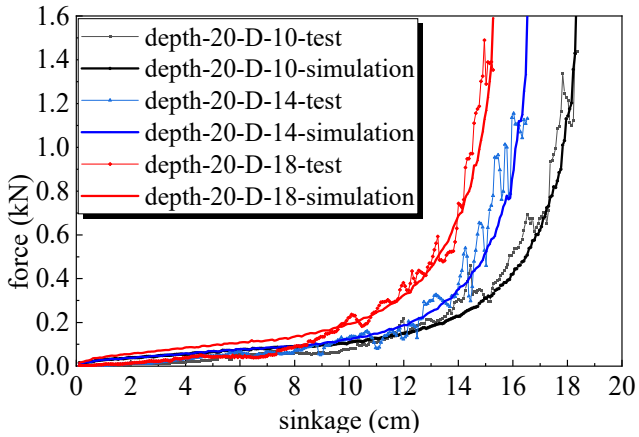
The parameters of the snow model obtained by inversion are shown in Table 3, on which the simulation of the load–sinkage relationship in different snow depths and different circular plate diameters was based. The simulation results were compared with the corresponding test data, and the results are shown in Figure 13.



(**a**) snow depth = 0.14 m



(**b**) snow depth = 0.18 m



(**c**) snow depth = 0.20 m

Figure 13. Comparison of load–sinkage results of snow using inversion results of snow material parameters (different snow depths and different plate diameters).

Table 3. Reversed parameters of snow plastic material model.

Elastic	**Young's modulus** E/(Pa)		**Poisson's ratio** ν	**Density** ρ/(kg·m^{-3})		
	1.669×10^6		0.3	325		
Plastic	**Cohesion** c/(Pa)	**Angle of friction** β/deg	**Cap eccentricity**	**Initial yield surface position** $\varepsilon_{vol}^{pl}\|_{initial}$	**Transition surface radius**	**Flow stress ratio**
	3587.35	12.1284	0.00011	0.001	0	1
Cap hardening				ε_{vol}^{pl}	**Mean hydrostatic pressure**/Pa	
				0	26.73	
				0.593	3995	
				0.669	7755	
				0.806	15,745	
				0.944	39,245	
				1.083	78,255	
				1.299	156,745	
				1.455	219,255	
				1.475	254,505	
				1.5	470,000	
				1.514	4,700,000	

The simulation results are consistent with the corresponding experimental results under different snow depths and different plate diameters. The correlation coefficient between the simulation results and experimental results is shown in Figure 14, and the minimum correlation coefficient is 0.8743, which is greater than 0.8. Therefore, the inversion results have a strong correlation with the experimental results.

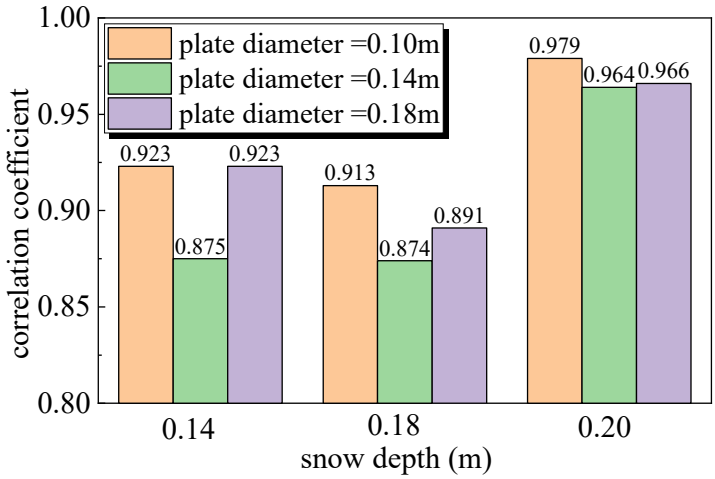


Figure 14. Correlation coefficient between simulation results and experimental data under different simulation conditions.

6. Conclusions

In this paper, the snow plastic model, the MDPC model, was analyzed. A simulation model of the load–sinkage relationship of snow under circular plate loading was established by using the coupled Eulerian–Lagrangian method. A single-factor sensitivity analysis of the snow parameters was carried out, and an in situ experiment of the load–sinkage

relationship was conducted. The parameter inversion of the snow model parameters was carried out by using the experimental results as the matching data, and the following conclusions were obtained:

(1) In the simulation of the large deformation of soft terrain such as snow, the mesh was seriously distorted when using the Lagrange method, resulting in the simulation being aborted. The CEL method is an effective method to simulate the large deformation of snow.

(2) The material cohesive, angle of friction, and hardening law of snow have a great influence on the load–sinkage relationship during continuous loading. The elastic modulus of snow has a great influence on the unloading stiffness of snow, while the Poisson's ratio and density have almost no influence on the bearing characteristics of snow.

(3) The parameter inversion of the snow model was carried out. The load–sinkage curve obtained by inversion had a good fit with the experimental data, and the correlation coefficient was 0.979.

(4) The simulation results of the load–sinkage relationship of snow under circular plate loading based on the snow parameters obtained by parameter inversion had a good fit with the experimental data with different plate diameters and snow depths. In the cases studied in this paper, the minimum correlation coefficient between the simulation results and the experimental results was 0.8743. The snow model parameters calibrated by parameter inversion were able to reflect the bearing characteristics of the experimental snow accurately.

In this paper, the snow parameters were inverted based on the in situ test results of the load–sinkage relationship of snow, and the simulation model of undisturbed snow was obtained. In the future, further in situ testing experiments will be conducted on the load–sinkage relationship of snow in different regions, at different depths, at different sintering times, and for different microscopic crystal structures. More experimental data will be used to verify the inversion results of the snow parameters, analyze the relationship between snow parameters and water content, temperature, light, crystal structure, etc., and build a snow parameter database. The performance of wheeled/tracked vehicles in different types of snow will be predicted by numerical simulation. Moreover, deep learning technology may have broad application prospects in the research of snow, including model parameter calibration, and will be very helpful in solving the existing key technical problems.

Author Contributions: Conceptualization, W.W.; Methodology, Y.S.; Software, P.L.; Formal analysis, D.L.; Resources, J.L.; Data curation, X.L.; Writing—original draft, Q.M.; Writing—review & editing, M.Z.; Project administration, Q.Y. All authors have read and agreed to the published version of the manuscript.

Funding: This research received no external funding.

Data Availability Statement: Data are contained within the article.

Conflicts of Interest: Authors Pengyu Li and Dongqing Li were employed by the company Harbin First Machinery Group Co., Ltd. The remaining authors declare that the research was conducted in the absence of any commercial or financial relationships that could be construed as a potential conflict of interest.

References

1. Hetherington, J.G. Tracked vehicle operations on sand—Investigations at model scale. *J. Terramech.* **2005**, *42*, 65–70. [CrossRef]
2. Zeng, H.X.W.; Xu, W.; Zang, M.; Yang, P. Experimental and numerical investigations of tractive performance of off-road tires on gravel terrain. *Int. J. Comput. Methods* **2020**, *8*, 1950055. [CrossRef]
3. Gheshlaghi, F.; El-Sayegh, Z.; Sharifi, M.; El-Gindy, M. Prediction and validation of terramechanics models for estimation of tyre rolling resistance coefficient. *Int. J. Veh. Syst. Model. Test.* **2020**, *1*, 71–82. [CrossRef]

4. El-Sayegh, Z.; El-Gindy, M. Modelling and prediction of tyre–snow interaction using finite element analysis–smoothed particle hydrodynamics techniques. *Proc. Inst. Mech. Eng. Part D J. Automob. Eng.* **2018**, *233*, 1783–1792. [CrossRef]
5. Bekakos, C. Analytical and Finite Element Modelling of the Dynamic Interaction Between Off-Road Tyres And Deformable Terrains. Doctoral dissertation. Ph.D. Thesis, Loughborough University, Loughborough, UK, 2017.
6. Li, J.; Sun, S.; Sun, C.; Liu, C.; Tang, W.; Wang, H. Analysis of Effect of Grouser Height on Tractive Performance of Tracked Vehicle under Different Moisture Contents in Paddy Soil. *Agriculture* **2022**, *12*, 1581. [CrossRef]
7. Abele, G.; Gow, A.J. *Compressibility Characteristics of Undisturbed Snow*; US Army Cold Regions Research and Engineering Laboratory: Hanover, Germany, 1975.
8. Perla, R.; Beck, T.M.H.; Cheng, T.T. The Shear Strength Index of Alpine Snow. *Cold Reg. Sci. Technol.* **1982**, *6*, 11–20. [CrossRef]
9. Malcolm, M. *A Review of Basic Snow Mechanics*; US Army Cold Regions Research and Engineering Laboratory: Hanover, Germany, 1974.
10. Alger, R.; Osborne, M. *Snow Characterization Field Data Collection Results*; Final Report no. ACA89-85-K-002; Keweenaw Research Center, Michigan Technological University, Houghton: Calumet, MI, USA, 1989; Volume 8.
11. Shoop, S. *Finite Element Modeling of Tire Terrain Interaction*; University of Michigan: Ann Arbor, MI, USA, 2001.
12. Haehnel, R.B.; Shoop, S.A. A macroscale model for low density snow subjected to rapid loading. *Cold Reg. Sci. Technol.* **2004**, *40*, 193–211. [CrossRef]
13. Lee, J.H. Finite element modeling of interfacial forces and contact stresses of pneumatic tire on fresh snow for combined longitudinal and lateral slips. *J. Terramech.* **2011**, *48*, 171–197. [CrossRef]
14. Lee, J.H. A new indentation model for snow. *J. Terramech.* **2009**, *46*, 1–13. [CrossRef]
15. Lee, J.H.; Liu, Q.; Zhang, T. *Predictive Semi-Analytical Model for Tire-Snow Interaction*; No. 2005-01-0932; SAE Technical Paper: Warrendale, PA, USA, 2005.
16. Choi, J.H.; Cho, J.R.; Woo, J.S.; Kim, K.W. Numerical investigation of snow traction characteristics of 3-D patterned tire. *J. Terramech.* **2012**, *49*, 81–93. [CrossRef]
17. Jasoliya, D.; Untaroiu, A.; Untaroiu, C. A review of soil modeling for numerical simulations of soil-tire/agricultural tools interaction. *J. Terramech.* **2024**, *111*, 41–64. [CrossRef]
18. Swamy, V.S.; Pandit, R.; Yerro, A.; Sandu, C.; Rizzo, D.M.; Sebeck, K.; Gorsich, D. Review of modeling and validation techniques for tire-deformable soil interactions. *J. Terramech.* **2023**, *109*, 73–92. [CrossRef]
19. Huang, F.; Zhuo, L.; Zhang, K. A Study on the Shear Strength Characteristic of Unsaturated Red Clay. *World J. Eng. Technol.* **2022**, *10*, 714–727. [CrossRef]
20. Zhu, J.; Zou, M.; Liu, Y.; Gao, K.; Su, B.; Qi, Y. Measurement and calibration of DEM parameters of lunar soil simulant. *Acta Astronaut.* **2022**, *191*, 169–177. [CrossRef]
21. Yao, L.; Zhu, Y.; Wang, Y.; Shi, D.; Pang, S. Research of tire-soil interaction based on FEM-DEM for small wheeled mobile platform in forest. *Adv. Eng. Softw.* **2024**, *196*, 103735. [CrossRef]
22. Zhu, M.; Cheng, X.; Zhang, G.; Pang, X.; Ss, D.; Liu, J. Parameter back-analysis of hardening soil model for granite residual soil and its engineering applications. *Rock Soil Mech.* **2022**, *43*, 1061–1072.
23. Liu, X.; Wang, X.; Ma, H. Study on back-analysis method of constitutive parameters for Duncan-Chang model based on in -situ pressuremeter tests. *Chin. J. Geotech. Eng.* **2004**, *26*, 601–606.
24. Rangeard, D.Y.; Hicher, P.; Zentar, R. Determining soil permeability from pressuremeter tests. *Int. J. Numer. Anal. Methods Geomech.* **2002**, *27*, 1–24. [CrossRef]
25. Yao, H.; Zhang, Y.; Jiang, L.; Ewe, H.; Ng, M. Snow Parameters Inversion from Passive Microwave Remote Sensing Measurements by Deep Convolutional Neural Networks. *Sensors* **2022**, *22*, 4769. [CrossRef]
26. Zhan, J.; Zhang, R.; Tu, J.; Lv, J.; Bao, X.; Xie, L.; Li, S.; Zhan, R. GNSS-IR Snow Depth Retrieval Based on the Fusion of Multi-Satellite SNR Data by the BP Neural Network. *Remote Sens.* **2022**, *14*, 1395. [CrossRef]
27. Li, H.; Schindler, C. Investigation of Tire-Soil Interaction with Analytical and Finite Element Method#. *Mech. Based Des. Struct. Mach.* **2013**, *41*, 293–315. [CrossRef]
28. Zeng, H.; Xu, W.; Zang, M.; Yang, P. Calibration of DEM-FEM model parameters for traction performance analysis of an off-road tire on gravel terrain. *Powder Technol.* **2020**, *362*, 350–361. [CrossRef]
29. Li, H.; Schindler, C. Analysis of soil compaction and tire mobility with finite element method. *Proc. Inst. Mech. Eng. Part K J. Multi-Body Dyn.* **2013**, *227*, 275–291. [CrossRef]
30. Hua, C.; Niu, R.; Kuang, X.; Yu, B.; Jiang, C.; Liu, W. Rapid and precise calibration of soil microparameters for high-fidelity discrete element models in vehicle mobility simulation. *J. Terramech.* **2024**, *115*, 100985. [CrossRef]
31. Zhou, L.; Gao, J.; Hu, C.; Li, Q. Numerical simulation and testing verification of the interaction between track and sandy ground based on discrete element method. *J. Terramech.* **2021**, *95*, 73–88. [CrossRef]
32. Fayun, L.; Yajie, J.; Yujin, D. Experimental study on parameters of HSS model for soft soils in Shanghai. *Chin. J. Geotech. Eng.* **2017**, *39*, 269–278.

33. Yan, Q.; Zhu, M.; Wei, W.; Liu, C.; Wang, M. Analysis of Contact Dynamics Characteristics of Tire-snow Interaction in Semi-infinite Snow Region. *Acta Armamentarii* **2024**, *45*, 925–933.
34. Wong, J.; Gaber, M. Theoretical prediction and experimental substantiation of the ground pressure distribution and tractive performance of tracked vehicles. *Proc. Inst. Mech. Eng. Part D Transp. Eng.* **1984**, *198*, 265–285. [CrossRef]
35. Helwany, S. *Applied Soil Mechanics with ABAQUS Applications*; John Wiley & Sons: Oxford, UK, 2007.
36. Zhu, M.; Yan, Q.; Wei, W.; Liu, C.; Wang, M.; Meng, Q.; Liu, J.; Li, P.; Li, D.; Peng, Q. Simulation on Vertical Displacement and Vertical Force Distribution of Snow Under Tracked Vehicle. In Proceedings of the Society of Automotive Engineers (SAE)-China Congress, Singapore, 21 February 2024; pp. 1493–1504.
37. Wang, P.; Lian, C.; Yue, C.; Wu, X.; Zhang, J.; Zhang, K.; Yue, Z. Experimental and numerical study of tire debris impact on fuel tank cover based on coupled Eulerian-Lagrangian method. *Int. J. Impact Eng.* **2021**, *157*, 103968. [CrossRef]
38. Zhang, L.; Cai, Z.; Wang, L.; Zhang, R.; Liu, H. Coupled Eulerian-Lagrangian finite element method for simulating soil-tool interaction. *Biosyst. Eng.* **2018**, *175*, 96–105. [CrossRef]

Disclaimer/Publisher's Note: The statements, opinions and data contained in all publications are solely those of the individual author(s) and contributor(s) and not of MDPI and/or the editor(s). MDPI and/or the editor(s) disclaim responsibility for any injury to people or property resulting from any ideas, methods, instructions or products referred to in the content.